Electronic Supporting Information

Supramolecular assembly of a hierarchically structured 3D potassium vanadate framework

Simon Greiner, Montaha Anjass,* and Carsten Streb*

1. Instrumentation

Single-crystal X-ray diffraction (scXRD) was measured on a Bruker D8 Quest Single-crystal X-ray diffractometer equipped with a graphite monochromator using $Mo_{K\alpha}$ radiation (wavelength $\lambda(Mo_{K\alpha})$ = 0.71073 Å).

Attenuated total reflectance-Fourier-transformed infrared spectroscopy (ATR-FT-IR) was recorded using a PerkinElmer Spectrum Two spectrometer in a range between 4000 and 500 cm^{-1}.

UV-vis spectroscopy was performed on a Varian Cary 50 spectrophotometer in a standard cuvette (d = 10.0 mm)

Inductively coupled plasma optical emission spectroscopy (ICP-OES) was performed on a Spectro Arcos FHS12.

Thermogravimetric analysis (TGA) was carried out on a NETZSCH TG 209F1 analyser at a heating rate of 10.0 K min^{-1} in a range between 30 and 700 °C under air in an Al crucible.

Mass spectrometry: Electrospray-ionization mass spectrometry (ESI-MS) was performed using Hybrid 7T FT-ICR Bruker solariX mass spectrometer in negative ion detection mode.

X-ray photoelectron spectroscopy (XPS) was performed on Physical Electronics PHI 5800 spectrometer using monochromatized $Al_{K\alpha}$ (1486.6 eV) radiation. The measurements were performed with a detection angle of 45 °C, using pass energies at the analyzer of 93.9 and 29.35 eV for survey and detail spectra, respectively. The samples were neutralized with electrons from a flood gun (current 3 µA) to compensate for charging effects at the surface.

Scanning Electron Microscopy (SEM) and **Energy-dispersive X-ray spectroscopy** (EDX) were performed on a Zeiss Gemini Leo 1550 VP equipped with a Silicon Drift Detector (OXFORD Instruments) using a 10 keV electron beam.

2. Experimental procedure

All chemicals were purchased from Sigma Aldrich, VWR or Alfa Aesar and were of reagent grade. The chemicals were used without further purification unless stated otherwise.

Synthesis $K_5(CH_3CN)_3[V_{12}O_{32}Cl]$ (= $\{K_5V_{12}\}$):

$(n Bu_4N)_3[(C_2H_8N)_2V_{12}O_{32}Cl] \cdot CH_3CN$[1] (240 mg, 0.12 mmol, 1 eq) and KSCN (94 mg, 0.96 mmol, 8 eq) were dissolved in acetonitrile (20 ml) and stirred at room temperature for 5 h. Diffusion crystallization of diethyl ether yielded fine, needle-shaped, yellow-greenish crystals.
Yield: 140 mg (94.8 µmol, 79% based on V).
Characteristic IR bands (in cm^{-1}): 3527 (b), 1947 (w), 1614 (m), 1462 (w), 1396 (w), 1363 (w), 986 (vs), 819 (s), 767 (s), 685 (s), 630 (vs).
UV/vis (in MeCN): ε_{244} = 63642 M^{-1} cm^{-1}, ε_{358} = 16906 M^{-1} cm^{-1}.
ICP-OES in wt.-% (calcd.): V 41.6 (41.4), K 12.9 (13.2). The ratio of K:V is 4.8 : 12.

3. Crystallographic section

Suitable single-crystals of **{K_5V_{12}}** were mounted onto a microloop using Fomblin oil. X-ray diffraction intensity data were measured on a Bruker D8 QUEST diffractometer λ($Mo_{K\alpha}$ = 0.71073 Å) equipped with a graphite monochromator. Structure solution was carried out using SHELX-2013[2] package through OLEX2[3] Corrections for incident and diffracted beam absorption effects were applied using empirical methods.[4] Structures were solved by a combination of direct methods and difference Fourier syntheses and refined against F^2 by the full matrix least-squares technique. Non-hydrogen atoms were refined anisotropically. Hydrogen atoms were added to carbon atoms using a riding model. The geometry and anisotropic refinement of the solvent and ligand molecules was restrained using SIMU and DELU. The vanadium oxo framework was refined fully anisotropically and no restraints were used. Note that the structure features disorder related to the solvent acetonitrile groups. The SQUEEZE[5] routine was applied to account for diffuse solvent molecules. The CIF file can be obtained free of charge from the CCDC.

Table S 1 Crystallographic parameters for **{K_5V_{12}}**.

Compound code	**{K_5V_{12}}**
CCDC code	2057315
Empirical formula	$C_{27}H_{40.5}Cl_2K_{10}N_{13.5}O_{64}V_{24}$
Formula weight / g mol^{-1}	3262.29
Temperature / K	150
Wavelength / nm	0.71073
Crystal system	Monoclinic
Space group	$P2_1/n$
Unit cell dimensions / Å	*a* = 13.0012(7), *b* = 20.1680(8), *c* = 38.2835(16)
Unit cell angles / °	α = 90, β = 93.6201(18), γ = 90
Volume / $Å^3$	10018.2(8)
Z	4
Density (calcd.) / g cm^{-3}	2.162
Absorption coefficient μ / mm^{-1}	2.689
F(000)	6334.0
2Θ range for data collection / °	3.732 to 52.79
Index ranges	-16 ≤ h ≤ 16, -25 ≤ k ≤ 25, -47 ≤ l ≤ 47
No. reflections	133193
Independent reflections	20491 [R_{int} = 0.1410, R_{sigma} = 0.0820]
Data / restraints / parameters	20491/218/1293
Goodness-of-fit	1.156
Final R indices [I>2sigma(I)]	R_1 = 0.0792, wR_2 = 0.1389
R indices (all data)	R_1 = 0.1005, wR_2 = 0.1469
Largest diff. peak and hole	1.36/-0.91

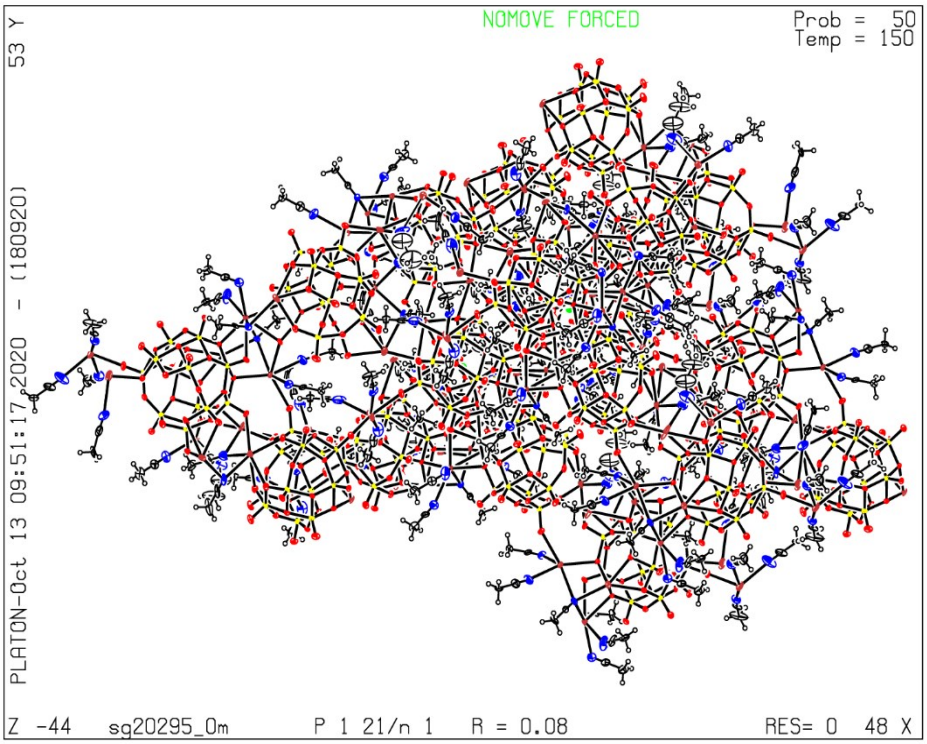

Figure S 1 ORTEP-representation of **{K_5V_{12}}**, probability ellipsoids shown at 50%.

4. Thermogravimetric Analysis

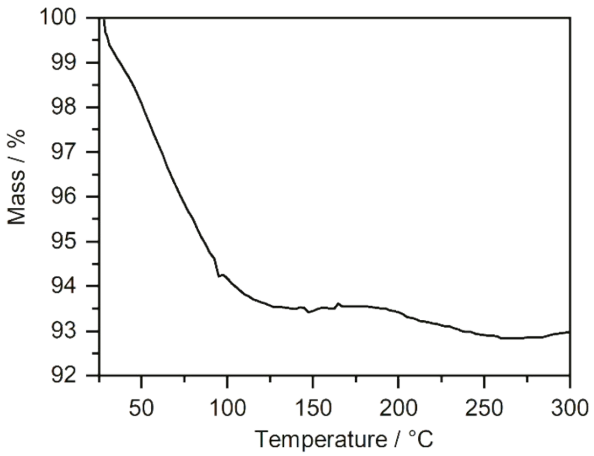

Figure S 2: Thermogravimetric analysis (under air) of **{K_5V_{12}}** showing a weight loss of ca. 6.5 wt.-% between 25 and 150 °C, corresponding to ca. 2.5 acetonitrile molecules (calc.: 6.9 wt.-%).

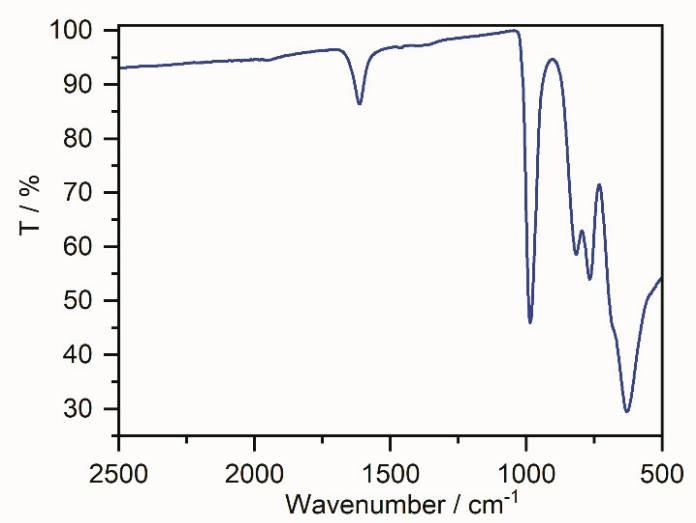

Figure S 3 ATR-FT-IR spectra of **{K_5V_{12}}**.

5. Infrared spectroscopy

6. X-ray photoelectron spectroscopy

From the fitting of the V 2p spectrum, the obtained binding energy values of **{K_5V_{12}}** are for V $2p_{3/2}$ 517.1 eV, V $2p_{1/2}$ 524.5 eV and a V $2p_{3/2}$ – V $2p_{1/2}$ splitting with 7.3 eV confirming all vanadium atoms in oxidation state +5 for **{K_5V_{12}}**.[6,7]

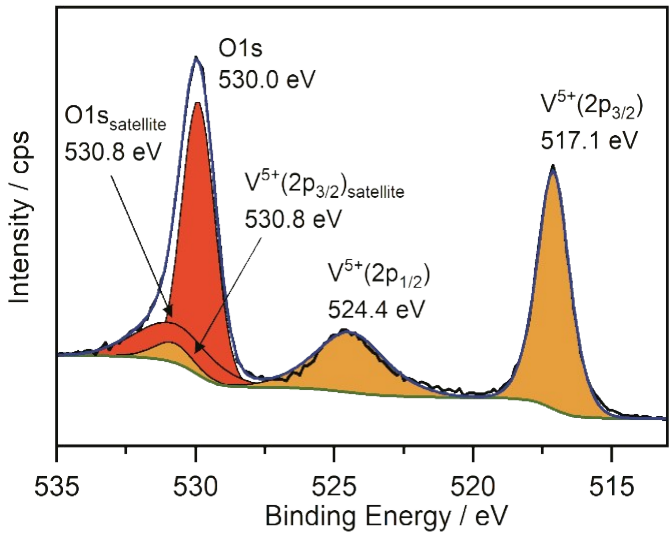

Figure S 4 XPS spectrum of **{K_5V_{12}}**.

7. UV/vis spectroscopy of $\{K_5V_{12}\}$

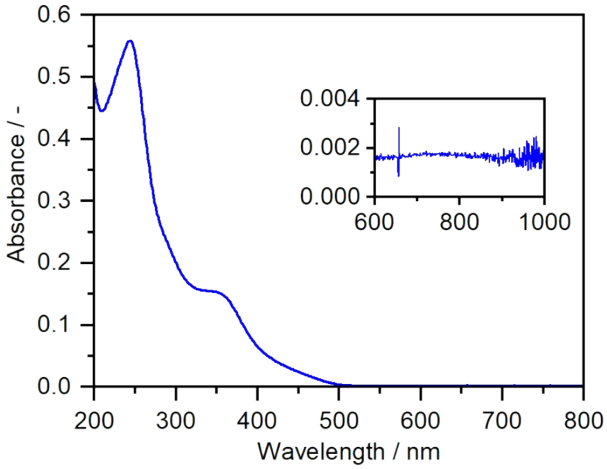

Figure S 5 UV/vis spectrum of **$\{K_5V_{12}\}$** in acetonitrile c = 9 x 10^{-6} M. Inset: magnified view of the 600-1000 nm range, where IVCT transitions for partially reduced vanadates would be observed. Note, that no IVCT absorption is detected.

8. Scanning Electron Microscopy

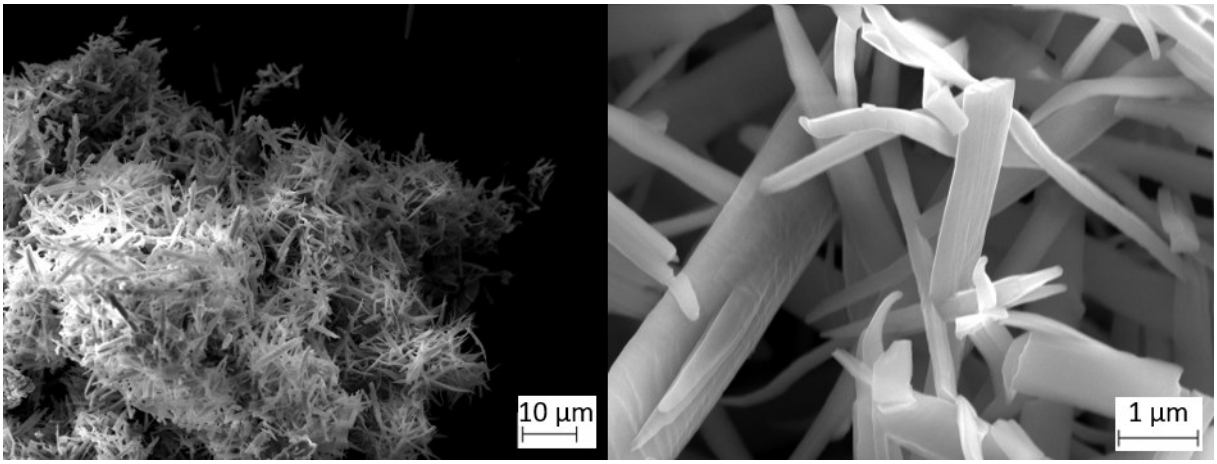

Figure S 6 Scanning Electron micrographs of **$\{K_5V_{12}\}$** at magnification of 1k (left) and 15k (right). Accelerating voltage: 10 keV.

9. Structural analysis of the metal binding site

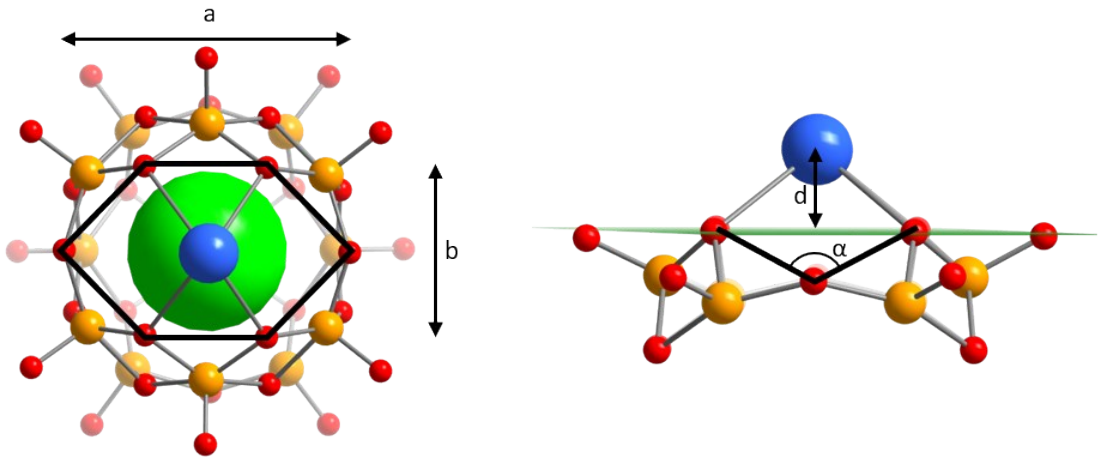

Figure S 7 Top view (left) and side view (right) of **{K_5V_{12}}**, showing the angle and distances in the hexagonal binding site. Color scheme: V: yellow; O: red; Cl: green; K: light blue.

Table S 2 Angles and distances of the hexagonal binding site of **{K_5V_{12}}** and related di-functionalized compounds.

	$(H_2NMe_2)_2\{V_{12}\}$[1]	**$\{Mn_2V_{12}\}$**[8]	**$\{Sr_2V_{12}\}x(C_5H_9NO)$**[9]	**$\{Ca_2V_{12}\}$**[10]	**$\{K_5V_{12}\}$**
d / Å	1.6	0.6	1.0	1.0	1.5
a / Å	6.0	6.5	6.0	6.3	6.2
b / Å	3.9	3.2	3.8	3.4	3.8
α / °	91	73	89	80	86

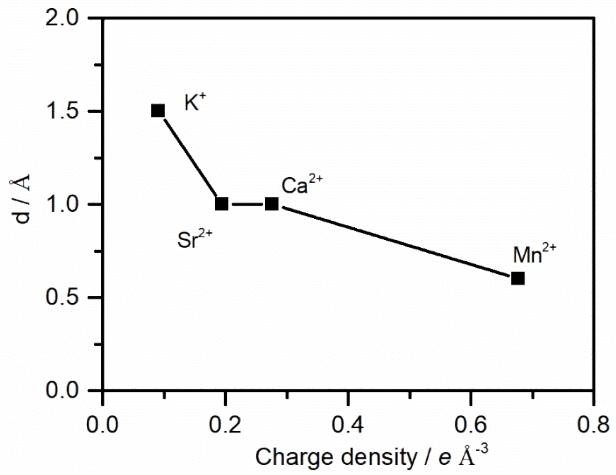

Figure S 8 Relationship between distance to the cluster and the charge density of selected di-functionalized $\{M_2V_{12}\}$ compounds (M = K^+, Sr^{2+}, Ca^{2+} and Mn^{2+}), showing increasing distance with lower charge density.

10. Mass spectrometry of $\{K_5V_{12}\}$

Table S 3 Potassium vanadate species observed in negative ion mode HR-ESI mass spectrometry of **$\{K_5V_{12}\}$**.

Observed m/z	Calculated m/z	Charge	Assignment
462.6543	462.6543	1-	$[V_5O_{13}]^{1-}$
536.5851	536.5868	1-	$\{K[V_5O_{13}Cl]\}^{1-}$
600.5437	600.5467	2- / 1-	$\{K_2[V_{12}O_{32}]\}^{2-}$ / $\{K[V_6O_{16}]\}^{1-}$
618.5339	618.5350	2-	$\{K_2H[V^V_{12}O_{32}Cl]\}^{2-}$
629.5247	629.5260	2-	$\{NaK_2[V^V_{12}O_{32}Cl]\}^{2-}$
637.5009	637.5130	2-	$\{K_3[V^V_{12}O_{32}Cl]\}^{2-}$
674.4764	674.4792	1-	$[K_2V_6O_{16}Cl]^{1-}$
845.0261	845.0284	3-	$\{NaHK_5[V^V_{12}O_{32}Cl]_2\}^{3-}$
850.3505	850.3530	3-	$\{HK_6[V^V_{12}O_{32}Cl]_2\}^{3-}$
857.6779	857.6803	3-	$\{Na_1K_6[V^V_{12}O_{32}Cl]_2\}^{3-}$
863.0009	863.0050	3-	$\{K_7[V^V_{12}O_{32}Cl]_2\}^{3-}$
966.2614	966.2620	4-	$\{HK_{10}[V^V_{12}O_{32}Cl]_3\}^{4-}$
971.7558	971.7575	4-	$\{NaK_{10}[V^V_{12}O_{32}Cl]_3\}^{4-}$
975.7510	975.7510	4-	$\{K_{11}[V^V_{12}O_{32}Cl]_3\}^{4-}$
1040.2039	1040.2038	5-	$\{NaK_{14}[V^V_{12}O_{32}Cl]_4\}^{5-}$
1043.3978	1043.3986	5-	$\{K_{15}[V^V_{12}O_{32}Cl]_4\}^{5-}$

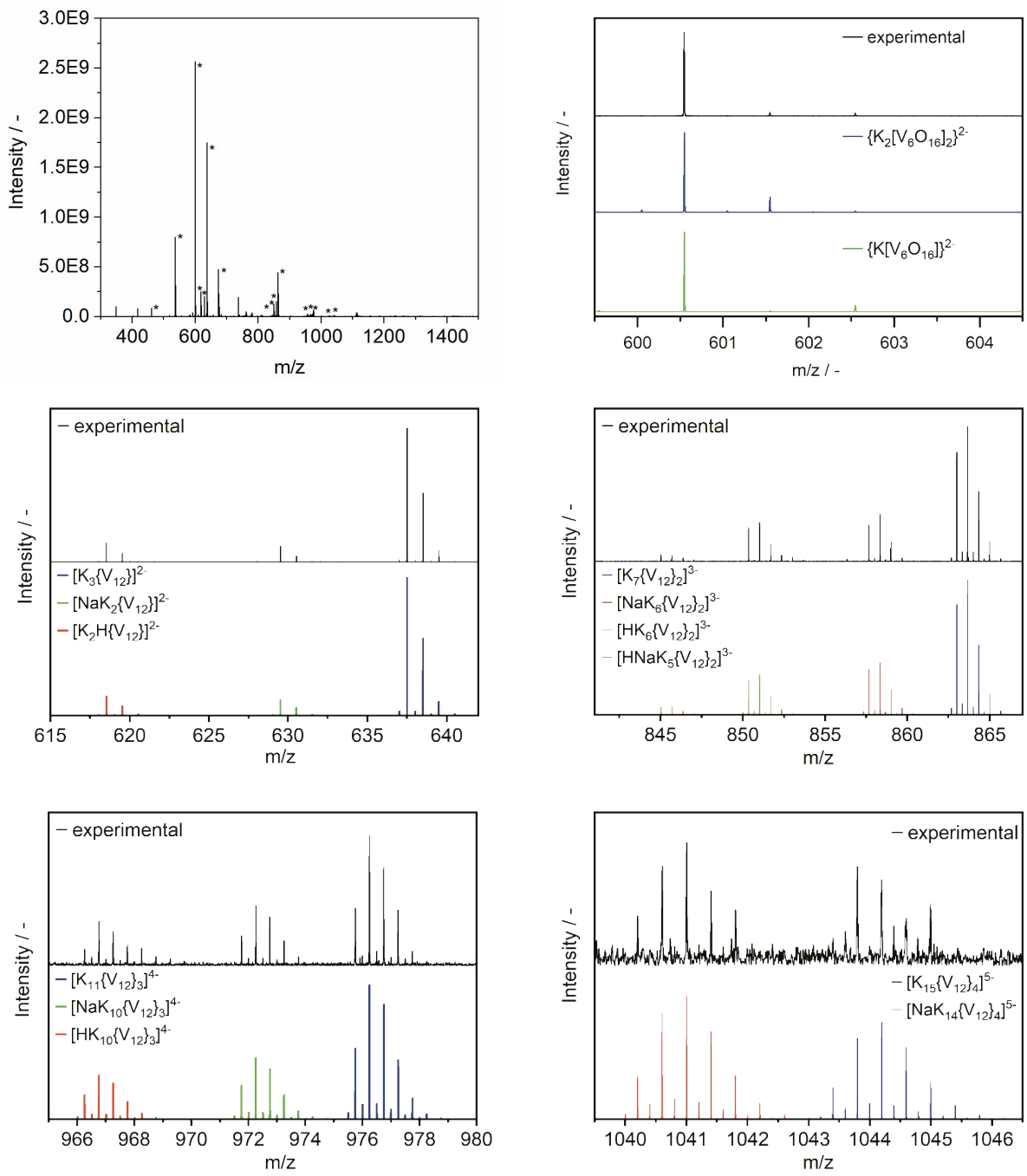

Figure S 9 Top left: High resolution electrospray ionization mass-spectrometry of **{K_5V_{12}}** (ca. $5x10^{-5}$ M in acetonitrile). **Top right:** Experimental and simulated ESI mass spectrum of the main peak assigned to a mixture of $\{K[V_6O_{16}]\}^{1-}$ and $\{K_2[V_6O_{16}]_2\}^{2-}$ observed at m/z = 600.5437. **Middle left:** Experimental and simulated spectrum of the series of the full cluster with stepwise replaced potassium ions $\{K_3[V_{12}O_{32}Cl]\}^{3-}$ observed at m/z = 637.5009. **Middle right:** Experimental and simulated ESI mass spectrum of the series of dimers with stepwise replaced potassium ions $\{K_7[V_{12}O_{32}Cl]_2\}^{3-}$ found at m/z = 863.0009. **Bottom left:** Experimental and simulated ESI mass spectrum of the series of trimers with stepwise replaced potassium ions $\{K_{11}[V_{12}O_{32}Cl]_3\}^{4-}$ found at m/z = 975.7510. **Bottom right:** Experimental and simulated ESI mass spectrum of fragments with four cluster units starting from $\{K_{15}[V_{12}O_{32}Cl]_4\}^{5-}$ found at m/z = 1043.3978.

11. References

1 K. Kastner, J. T. Margraf, T. Clark and C. Streb, *Chem. - A Eur. J.*, 2014, **20**, 12269–12273.

2 George M. Sheldrick, *Acta Crystallogr. Sect. C*, 2015, **71**, 3–8.

3 O. V. Dolomanov, L. J. Bourhis, R. J. Gildea, J. A. K. Howard and H. Puschmann, *J. Appl. Crystallogr.*, 2009, **42**, 339–341.

4 B. Y. R. H. Blessing, *Acta Crystallogr. Sect. A*, 1995, **51**, 33–38.

5 A. L. Spek, *Acta Crystallogr. Sect. C Struct. Chem.*, 2015, **71**, 9–18.

6 G. Silversmit, D. Depla, H. Poelman, G. B. Marin and R. De Gryse, *J. Electron Spectros. Relat. Phenomena*, 2004, **135**, 167–175.

7 E. Hryha, E. Rutqvist and L. Nyborg, *Surf. Interface Anal.*, 2012, **44**, 1022–1025.

8 K. Kastner, J. Forster, H. Ida, G. N. Newton, H. Oshio and C. Streb, *Chem. - A Eur. J.*, 2015, **21**, 7686–7689.

9 B. Schwarz, M. Dürr, K. Kastner, N. Heber, I. Ivanović-Burmazović and C. Streb, *Inorg. Chem.*, 2019, **58**, 11684–11688.

10 S. Greiner, B. Schwarz, M. R. Ringenberg, M. Dürr, I. Ivanovic-Burmazovic, M. Fichtner, M. Anjass and C. Streb, *Chem. Sci.*, 2020, **11**, 4450–4455.

12. Author Contributions

All authors conceived the study. S. G. performed synthesis, characterization, and data analysis. S. G., M. A. and C. S. wrote the manuscript.